

1 **Kaposi sarcoma-associated herpesvirus infection in HIV patients: potential**
2 **role of HIV-associated extracellular vesicles**

3

4 Lechuang Chen^{1,¶}, Zhimin Feng^{1,¶}, Guoxiang Yuan^{1,¶}, Benjamin Reinthal¹, Fengchun Ye^{2,3}, Ge
5 Jin^{1,3,4,*}

6

7 ¹Department of Biological Sciences, Case Western Reserve University School of Dental
8 Medicine, Cleveland, Ohio, United States of America

9 ²Department of Molecular Biology and Microbiology, Case Western Reserve University School
10 of Medicine, Cleveland, Ohio, United States of America

11 ³Center for AIDS Research, Case Western Reserve University and University Hospitals
12 Cleveland Medical Center, Cleveland, Ohio, United States of America

13 ⁴Case Comprehensive Cancer Center, Case Western Reserve University School of Medicine,
14 Cleveland, Ohio, United States of America

15

16 *Corresponding author

17 Email: ge.jin@case.edu (GJ)

18

19 ¶These authors also contributed equally to this work.

20

21

22

23

24

25 **Abstract**

26 Kaposi sarcoma-associated herpesvirus (KSHV) is the causal agent for Kaposi sarcoma
27 (KS), the most common malignancy in people living with HIV/AIDS. The oral cavity is a major
28 route for KSHV infection and transmission. However, how KSHV breaches the oral epithelial
29 barrier for spreading to the body is not clear. Here we show that extracellular vesicles (EVs)
30 purified from saliva of HIV-positive individuals and secreted by HIV-1-infected T cells promote
31 KSHV infectivity in both monolayer and 3-dimensional models of immortalized and primary
32 human oral epithelial cells, establishing the latency of the virus. The HIV trans-activation
33 response (TAR) element RNA in HIV-associated EVs contributes to the infectivity of KSHV
34 through the epidermal growth factor receptor (EGFR). Cetuximab, a monoclonal neutralizing
35 antibody to EGFR, blocks HIV-associated EV-enhanced KSHV infection. Our findings reveal
36 that saliva containing HIV-associated EVs is a risk factor for enhancement of KSHV infection
37 and that inhibition of EGFR serves as a novel strategy for controlling KSHV infection and
38 transmission in the oral cavity.

39

40 **Author summary**

41 Kaposi sarcoma-associated herpesvirus (KSHV) is a causal agent for Kaposi sarcoma
42 (KS), the most common malignancy in HIV/AIDS patients. Oral transmission through saliva is
43 considered the most common route for spreading of the virus among HIV/AIDS patients.
44 However, the role of HIV-specific components in co-transfection of KSHV is unclear. We
45 demonstrate that extracellular vesicles (EV) purified from saliva of HIV patients and secreted by
46 HIV-infected T cells promote KSHV infectivity in immortalized and primary oral epithelial cells.

47 HIV-associated EVs promote KSHV infection depends on the HIV trans-activation element
48 (TAR) RNA and EGFR of oral epithelial cells, both can be targeted for reducing KSHV infection.
49 These results reveal that HIV-EVs is a risk factor for KSHV co-infection in the HIV-infected
50 population.

51 52 **Introduction**

53 Kaposi sarcoma (KS), the most common malignancy in patients infected with HIV, is
54 etiologically associated with infection by Kaposi sarcoma-associated herpesvirus (KSHV), also
55 known as human herpesvirus 8 (HHV-8) [1]. This oncogenic gamma-herpesvirus is also linked
56 with primary effusion lymphoma (PEL), multicentric Castleman’s disease (MCD), and KSHV
57 inflammatory cytokine syndrome (KICS) in aging people and immune compromised adults [2].
58 Oral transmission of KSHV through saliva in particular is believed to be the most common route
59 for spreading of the virus among homosexual people and “mother to child” transmission [3,4].
60 The oral mucosa has shown to be the first target of KSHV infection once the virus is in the oral
61 cavity [5,6,7,8,9]. Although KS incidence has dramatically decreased in developed countries in
62 the era of antiretroviral therapy (ART), KS remains the most frequent tumor in the HIV-infected
63 population worldwide [10,11,12]. The oral milieu of HIV-infected patients has long been
64 deduced to favor KSHV infection; however, the role of HIV in KSHV infection and transmission
65 is largely unknown.

66
67 Most types of cells can release lipid membrane-enclosed vesicles, generally called
68 extracellular vesicles (EVs), into the extracellular space and body fluids. Saliva and other body
69 fluids contain a variety of EVs [13,14,15,16]. EVs are highly heterogeneous and dynamic and

70 can be generally grouped into exosomes [17,18,19,20], macrovesicles [21], and apoptotic bodies
71 based on biogenesis and the origin of vesicles [22]. EVs contain molecular components of their
72 cells of origin, including proteins and RNAs, to play roles in intercellular communication,
73 molecular transfer, and immune regulation at local and distant sites [13,20,23]. EVs derived from
74 culture supernatants of latently HIV-1-infected T-cell clones do not contain HIV-1 viral
75 particles, although these EVs do contain viral proteins such as Gag and the precursor form of
76 Env protein (p160) [24]. The HIV transactivation response (TAR) element RNA, a precursor of
77 several HIV-encoded miRNAs, can fold in the nascent transcript and facilitate binding of the
78 viral transcriptional trans-activator (Tat) protein to enhance transcription initiation and
79 elongation of HIV [25]. EVs isolated from HIV-1-infected cells or from HIV-positive patient
80 sera contain TAR RNA in vast excess of total viral RNA [24,26]. TAR RNA-bearing EVs can
81 induce proinflammatory cytokines in primary macrophages [27] and stimulate proliferation,
82 migration and invasion of head and neck and lung cancer cells in an epidermal growth factor
83 receptor (EGFR)-dependent manner [26]. EVs in body fluids of HIV/AIDS patients may
84 mediate HIV-1 RNA and protein trafficking and affect HIV pathogenesis [28,29]. However, the
85 role of salivary HIV-associated EVs in co-infection of KSHV has not been explored [29].

86

87 Here, we report that EVs purified from the saliva of HIV-infected patients and secreted
88 from culture medium of latently HIV-infected T cells enhance KSHV infectivity in human oral
89 epithelial cells cultured in both monolayer and 3-dimensional (3-D) formats. EVs from T cells
90 infected with an HIV-1 provirus, which contains a dysfunctional mutant HIV Tat and lack of the
91 Nef gene, can still stimulate KSHV infection. Although HIV-associated (HIV+) EVs lack viral
92 proteins that are involved in cellular processes; they contain the HIV TAR RNA in excess of

93 other HIV RNAs. We demonstrate that TAR RNA alone and TAR RNA-bearing EVs are able to
94 enhance KSHV infectivity in oral epithelial cells, indicating the importance of the HIV TAR
95 RNA in promoting KSHV infection. HIV+ EV-enhanced KSHV infection is blocked by the
96 monoclonal antibody against EGFR. Our findings reveal that HIV+ saliva EVs is a risk factor for
97 enhancement of KSHV infection and that inhibition of EGFR serves as a novel strategy for
98 potentially controlling KSHV infection and transmission in the oral cavity.

99

100 **Results**

101 **HIV-associated EVs enhance KSHV infectivity in oral epithelial cells.** We treated iSLK-
102 BAC16 cells with sodium butyrate and doxycycline to produce infectious KSHV virions, which
103 contain a green fluorescent protein (GFP) cassette for monitoring success infection in target cells
104 [30]. To determine the multiplicity of infection (MOI) for each of KSHV stocks, we infected the
105 immortalized oral epithelial line OKF6/TERT2 [31] using each KSHV preparation at various
106 dilutions for 24 hr, followed by immunofluorescent staining of cells for KSHV-specific markers.
107 We found that KSHV infected OKF6/TERT2 cells, leading to expression of the KSHV latency-
108 associated nuclear antigen (LANA) and GFP and that 1:100 dilution of the KSHV stocks was
109 estimated to equal to MOI 0.1, which was used throughout all the experiments to ensure consistent
110 results (S1 Fig).

111

112 To determine whether HIV+ EVs were able to affect KSHV infection in oral epithelial
113 cells, we incubated OKF6/TERT2 cells with KSHV virions in the presence of EVs isolated from
114 culture supernatants of latently HIV-1-infected J1.1 T cells or control “virus-free” Jurkat cells

115 [26,32]. HIV+ EVs from J1.1 cells significantly enhanced KSHV infection compared to those
116 isolated from control Jurkat T cells as determined by immunofluorescence microscopy of LANA
117 and GFP proteins (Fig 1A) and flow cytometry on GFP of infected cells (Fig 1B and 1C),
118 suggesting that HIV+ EVs potentially stimulated KSHV infectivity in oral epithelial cells. KSHV
119 infects the oral cavity and oropharynx and the infection is more prevalent in HIV-positive people
120 than that in the general population [6,33]. We postulated that saliva EVs in people living with
121 HIV might be responsible for the higher KSHV infection in HIV patients. To test this hypothesis,
122 EVs were purified from the saliva of HIV-infected donors and healthy individuals using the
123 differential ultracentrifugation protocol [26]. To determine whether EVs prepared from saliva
124 met the minimal requirement for EVs [34], we conducted immunoblotting on total saliva EVs.
125 Saliva EVs from both HIV+ and HIV- donors contained tetraspanin proteins CD63, CD9 and
126 CD81 (Fig 2A), suggesting presence of exosomes in the EV preparations [34]. In addition, the
127 total EV protein amount was proportionally increased as more saliva was used in EV
128 purifications (S2 table), indicating our protocol was able to purified EVs from saliva samples
129 [34]. To determine whether HIV+ saliva EVs had HIV-specific components, we performed RT-
130 PCR on total EV RNA and found that only HIV+ saliva EVs contained HIV TAR, Tat and Nef
131 RNA, but not Env RNA (Fig 2B) [26], indicating that saliva of HIV-infected people contained
132 HIV+ EVs. To evaluate the effect of saliva EVs on KSHV infection, we infected OKF6/TERT2
133 cells with KSHV in the presence of EVs from saliva of HIV-infected subjects and control people,
134 respectively. Saliva EVs from HIV-infected subjects (Fig 2C, P8 and P9) significantly enhanced
135 KSHV infection in OKF6/TERT2 cells compared to EVs from the saliva of healthy individuals
136 (Fig 2C, N1 and N3) as determined by GFP flow cytometry. To determine whether KSHV was
137 able to infect primary human oral epithelial cells (HOECs), we treated the cells with KSHV

138 virions and found that KSHV-infected HOECs and infected cells expressed KSHV LANA and
139 GFP (Fig 2D), indicating that KSHV can infect primary oral epithelial cells. To test whether
140 HIV+ EVs were able to stimulate KSHV infection in these cells, we treated HOECs with EVs
141 from J1.1 and Jurkat cells as well as those purified from saliva of HIV+ or HIV- donors. EVs
142 isolated from HIV+ T cells or purified from the saliva of HIV-infected donors significantly
143 stimulated KSHV infection in HOECs compared to EVs from control T cells and saliva of
144 healthy donors, respectively (Fig 2E). To verify the stimulatory effect of HIV+ saliva EVs on
145 KSHV infection, we treated HOECs with saliva EVs derived from HIV-infected donors ($n=8$),
146 who were under ART treatment with CD4⁺ T-cell counts over 200 per ml, or those from healthy
147 individuals, followed by the KSHV infection assays. HIV+ saliva EVs considerably enhanced
148 KSHV infection compared to HIV- saliva EVs in primary HOECs (Fig 2F and 2G). Collectively,
149 these results demonstrate that HIV+ saliva EVs indeed promote KSHV infection in oral
150 epithelial cells.

151

152 **HIV+ saliva EVs stimulate KSHV infection and transmission in 3-D culture models of oral**
153 **mucosa.** The oral mucosa is the first target of KSHV infection once the virus is in the oral cavity
154 [6,7,8,9]. To evaluate the initial infection process of oral mucosa by KSHV, we created the 3-
155 dimensional (3-D) organotypic culture by using OKF6/TERT2 cells as described previously [35]
156 (Fig 3A), followed by KSHV infection. KSHV infected all layers of cells of the 3-D cultures of
157 OKF6/TERT2 cells in the presence of HIV+ EVs from J1.1 T cells; however, the infection was
158 barely detected in the presence of Jurkat cell EVs (Fig 3B). Further, we used 3-D cultured oral
159 buccal mucosal tissues consisting of primary human oral epithelial cells (MatTek Co., Ashland,
160 MA) (Fig. 3A, lower panel). EVs from HIV+ J1.1 T cells increased expression of KSHV LANA

161 protein (Fig 3C, arrowheads) and GFP (Fig 3C, arrows) upon KSHV infection in the mucosal
162 tissues and cells in the basal layers compared with HIV- EVs from Jurkat cells. Quantification of
163 Fig 3C demonstrated that HIV+ J1.1 T-cell EVs significantly increased KSHV-infected LANA-
164 expressing cells compared to HIV- Jurkat T-cells EVs (Fig 3D). Our findings suggested that
165 HIV+ EVs were able to facilitate KSHV transmission through oral mucosa.

166

167 **HIV transactivation element RNA (TAR) is critical for promoting KSHV infection.** We
168 suspected that HIV-specific EV cargo components were responsible for HIV+ EV-enhanced
169 KSHV infection in oral epithelial cells. Latently HIV-infected J1.1 T-cell EVs do not contain
170 HIV-1 viral particles, although these EVs have viral proteins such as Gag and the precursor form
171 of Env protein (p160) [24]. To determine if HIV+ EVs contained viral proteins, such as Tat and
172 Nef that are known to contribute to cellular functions [36,37], we performed immunoblot on total
173 EV proteins isolated from latently HIV-infected J1.1 cells and the HIV+ Jurkat clone C22G cell
174 line that contains a disruptive HIV *tat* mutant and *nef* deletion [38]. While the whole protein
175 lysates of HIV-infected J1.1 cells contained Tat and Nef proteins, EVs from J1.1 and C22G cells
176 did not produce the HIV proteins (Fig 4A), suggesting that the HIV-associated proteins might
177 not play a major role in promoting KSHV infection. We have reported that EVs from both J1.1
178 and C22G cell lines contain HIV TAR RNA, which is required for HIV+ EV-enhanced
179 proliferation of cancer cells [26]. HIV+ saliva EVs also contained TAR RNA (Fig 2B).
180 Therefore, we postulated that the TAR RNA-bearing EVs contributed to increase KSHV
181 infection in oral epithelial cells. To test this hypothesis, we treated OKF6/TERT2 cells with EVs
182 derived from J1.1 and C22G cells, respectively, followed by KSHV infection. HIV+ EVs from
183 both J1.1 and C22G cell lines promoted KSHV infectivity in OKF6/TERT2 cells as shown by

184 GFP flow cytometry (Fig 4B), suggesting that the TAR RNA contributed to HIV+ EV-enhanced
185 KSHV infectivity. HIV TAR RNA can directly induce expression of pro-oncogenes and
186 proliferation of cancer cells and the pro-tumor effect of TAR RNA requires the bulge-loop
187 structure [39] of the molecule [26]. To determine whether the bulge-loop structure of the TAR
188 RNA affected KSHV infection, we transfected OKF6/TERT2 cells with a TAR RNA mutant
189 containing 5 nucleotide replacements in bulge and loop sequences [26] and found that, while the
190 wild type TAR RNA promoted KSHV infection in oral epithelial cells, the mutant TAR RNA
191 failed to affect KSHV infection (Fig 4C, TAR vs. mut TAR). In addition, the RNA aptamer R06,
192 which is complementary to the TAR apical region and blocks TAR function without disrupting
193 the secondary structure of TAR [40], blocked TAR RNA-enhanced KSHV infection in
194 OKF6/TERT2 cells (Fig 4C, TAR+R06). However, a scrambled aptamer [26] did not
195 significantly change TAR RNA-induced KSHV infectivity (Fig 4C, TAR+scrb). These results
196 indicate that the bulge-loop region of TAR RNA is critical for its function associated with the
197 enhancement of KSHV infection in oral epithelial cells by TAR RNA-bearing EVs.

198

199 **HIV-associated EVs promote KSHV infectivity in an EGFR-dependent fashion.** We have reported
200 that EVs released from HIV-infected T cells and purified from plasma of HIV-positive patients
201 stimulate proliferation of HNSCC and lung cancer cells in an EGFR-dependent manner through
202 phosphorylation of ERK1/2 [26]. We reasoned that HIV+ EVs might promote KSHV infection
203 in oral epithelial cells via the similar mechanism. Indeed, treatment of OKF6/TERT2 cells with
204 cetuximab, a monoclonal antibody that blocks ligand binding to EGFR, inhibited KSHV
205 infection in OKF6/TERT2 cells as shown by reduced numbers of GFP+ cells in the culture (S3
206 Fig, HIV+ J1.1 EVs vs. +cetuximab). The inhibitory effect of cetuximab on HIV+ EV-enhanced

207 KSHV infection in OKF6/TERT2 cells was also determined by flow cytometry (Fig 5A). To
208 determine whether viral proteins defining KSHV productive infection were affected by inhibition
209 of EGFR, we treated OKF6/TERT2 cells with cetuximab and AG1478, a selective inhibitor of
210 EGFR phosphorylation [41], followed by KSHV infection assays in the presence and absence of
211 HIV+ EVs. HIV+ EVs enhanced expression of viral LANA and K8 proteins, an early viral
212 protein encoded by open reading frame K8 to regulate viral and host cell transcription [42,43].
213 However, expression of the viral proteins was blocked by cetuximab and AG1478 (Fig 5B).
214 Cetuximab also blocked HIV+ EV-enhanced KSHV infection in primary oral epithelial cells (Fig
215 5C). To determine whether inhibition of EGFR affected KSHV infection promoted by HIV+
216 saliva EVs in oral mucosal tissues, we treated the 3-D oral mucosal tissues with cetuximab,
217 followed by KSHV infection in the presence of HIV+ saliva EVs. While HIV+ saliva EVs
218 stimulated KSHV infection in oral mucosal tissues, cetuximab blocked the pro-infection effect of
219 HIV+ saliva EVs in the tissues (Fig 5D). Our findings indicate that blocking EGFR was able to
220 inhibit KSHV infection mediated by HIV+ EVs in the oral cavity.

221
222 **HIV-associated EVs stimulate p38 MAPK signaling through EGFR.** We have reported that
223 HIV+ EVs induce phosphorylation of ERK1/2 in an EGFR-dependent manner without causing
224 activation of the receptor in cancer cells [26]. To determine if HIV+ EVs contribute to activation
225 of EGFR and its down-stream effector kinases, we treated OKF6/TERT2 cells and HOECs with
226 EVs isolated from HIV+ J1.1 T cells and control Jurkat cells, respectively. Treatment of
227 OKF6/TERT2 cells with HIV+ EVs for 10 min induced phosphorylation of p38 MAPK, a
228 process was blocked by cetuximab and AG1478 (Fig 6A). Similarly, HIV+ EVs induced
229 phosphorylation of p38 MAPK, but not ERK1/2, in HOECs (Fig 6B). However, HIV+ EVs

230 failed to phosphorylate EGFR at tyrosine residuals 1068 (Y1068) and Y1173 in OKF6/TERT2
231 cells and HOECs, while EGF induced phosphorylation of EGFR at Y1068 and Y1173 as well as
232 phosphorylation of p38 MAPK and ERK1/2 in OKF6/TERT cells and HOECs, indicating that
233 the non-cancerous oral epithelial cells responded to EGF signaling (Fig 6A and 6B). In addition,
234 HIV+ EVs and EGF failed to phosphorylate STAT3, a downstream effector in the EGFR
235 signaling [44,45]. Our findings suggested that HIV+ EVs enhanced KSHV infection in an
236 EGFR-dependent manner possibly through activation of the EGFR/p38 signaling in oral
237 epithelial cells.

238

239 **Discussion**

240 HIV-infection is essential for KSHV co-infection, transmission, and its progression to
241 malignancies [46]. In people living with HIV/AIDS, co-infection with KSHV is much more
242 likely to lead to the development of KS and other KSHV-associated diseases [47,48,49]. The
243 incidence rates of KSHV detection are more prevalent in the HIV-infected population than that
244 in the general population in a case control study [33]. In this report, we demonstrate that HIV+
245 EVs from the saliva of HIV-positive patients and culture medium of HIV-infected T cells
246 promote KSHV productive infection in oral epithelial cells cultured in both monolayer and 3-D
247 models, indicating that HIV+ EVs are capable of regulating the initial steps of KSHV infection
248 in the oral cavity. Saliva-mediated oral transmission of KSHV is considered as the most common
249 route for spreading among homosexual people through deep kissing and “mother to child”
250 transmission [3,4,5,6,7,8,9]. Because both saliva and peripheral blood samples [26] from HIV-
251 infected persons contain HIV+ EVs, our findings suggest that the in HIV seropositive people
252 bear higher risk for KSHV infection most likely through EVs in the body fluids.

253

254 It has been reported that oral microbial metabolites contribute to infection and lytic
255 activation of KSHV [50,51,52]. Supernatants of periodontopathic bacteria cultures induce KSHV
256 replication in BCBL-1, a latently infected KSHV-based lymphoma-derived cell line, and
257 infection in embryonic kidney epithelial cells, human oral epithelial cells and umbilical vein
258 endothelial cells [51,52]. The saliva of patients with severe periodontal disease contain high
259 levels of short chain fatty acids that stimulate lytic gene expression of KSHV in a dose-
260 dependent fashion in BCBL-1 cells [52]. These bacterial metabolic products can stimulate
261 KSHV replication in infected cells using different mechanisms [51,52]. However, it is not clear
262 whether these microbial metabolic products are responsible for KSHV infection in HIV-infected
263 persons in the oral cavity. Collectively, our findings and these previous reports denote that
264 multiple microbial/viral risk factor contribute to KSHV pathogenesis in the oral cavity.

265

266 We have reported that HIV+ EVs stimulate proliferation and proto-oncogene expression
267 of squamous cell carcinoma cells in an EGFR-dependent manner [26]. Similarly, EGFR is
268 critical for HIV+ EV-enhanced KSHV infectivity; blocking the receptor with a neutralizing
269 antibody effectively inhibits KSHV infection in primary and immortalized oral epithelial cells.
270 EGFR mediates HIV+ EV entry into target cells and participates in EV-induced signaling,
271 including phosphorylation of ERK1/2, in head and neck as well as lung cancer cells [26].
272 However, cancer cells lacking EGFR, such as B-cell lymphoma cells, do not respond to HIV+
273 EVs [26]. Our results suggest that HIV+ EVs specifically promote KSHV infectivity through
274 EGFR in epithelial cells in the oral cavity.

275

276 EVs from plasma of HIV-infected people and culture supernatants of HIV-infected T
277 cells contain HIV TAR RNA in vast excess over all viral mRNAs [24,26]. In patients with
278 virtually undetectable virion levels, TAR RNA can still be found in blood EVs [27]. Our results
279 show that HIV+ saliva EVs contained TAR RNA and that synthetic TAR RNA considerably
280 increases KSHV infection in oral epithelial cells. Several reports have shown that the HIV TAR
281 RNA is a critical component of the HIV+ EV cargo and induces expression of proinflammatory
282 cytokines and proto-oncogenes in primary human macrophages and head and neck cancer cells,
283 respectively [24,26,27]. Synthetic TAR RNA alone can stimulate proliferation and migration of
284 head and neck cancer cells [26]. The mutant TAR RNA with 5-nucleotide substitutions in the
285 bulge and loop sequences fails to induce gene expression in head and neck cancer cells [26].
286 Similarly, our results demonstrate that the same TAR RNA mutant cannot enhance KSHV
287 infection in oral epithelial cells. In addition, the R06 nucleotide aptamer, which creates an
288 imperfect hairpin to complement to the entire TAR loop to block the function of TAR RNA [40],
289 blocks TAR RNA-induced KSHV infection in oral epithelial cells. The R06 aptamer and its
290 derivatives are able to reduce HIV-1 infection and inhibit the viral transcription [53,54]. Kolb *et*
291 *al.* have reported that the replication of HIV-1 and the activity of β -galactosidase under the
292 control of the HIV-1 5'LTR were reduced in cells expressing the nucleolar R06 transcript [53],
293 suggesting the antiviral activity of the nucleotide aptamer. Our results implicate that the R06
294 RNA aptamer and its functional derivatives can be potentially developed as a strategy for
295 controlling co-infection of the herpesvirus in the HIV-infected population.

296

297 We have reported that HIV+ EVs activate the ERK1/2 signaling through the EGFR-TLR3
298 axis to induce proto-oncogene expression and proliferation of head neck and lung cancer cells

299 [26]. However, our data show that HIV+ EVs specifically activate the MAPK p38, but not
300 ERK1/2, through EGFR without inducing phosphorylation of the receptor in non-cancerous oral
301 epithelial cells. Inhibition of the catalytic activity of the phosphorylated p38 blocks KSHV
302 reactivation, possibly through reduction in a global H3 acetylation and phosphorylation [55].
303 Various chromatin-silencing mechanisms, including histone deacetylation, repressive histone
304 methylation, and DNA methylation, lead to silence of the genomes of herpesviruses and HIV
305 during latency [56]. Multiple short chain fatty acids, including butyric acid, propionic acid,
306 isovaleric acid, and isobutyric acid, inhibit class-1/2 histone deacetylases (HDACs) for histone
307 hyperacetylation, resulting in expression of genes associated with the fate of KSHV infection and
308 viral reactivation [57,58,59]. The epigenetic modifications, particularly acetylation of histones,
309 are required for maintenance of KSHV latency in classic and AIDS-associated KS tissues [59].
310 Taken together, our findings provide an insight into the mechanisms underlying HIV-specific
311 components and co-infection of KSHV in people living with HIV/AIDS through the oral cavity.
312 In addition, targeting the HIV TAR RNA and EGFR of oral epithelial cells may serve as novel
313 approaches to control KSHV infection in the HIV-infected population.

314

315 **Materials and methods**

316 **Ethical statement**

317 For all human subject studies, written informed consent was obtained from all study participants
318 according to protocol approved by the Human Subjects Institutional Review Board (IRB) at Case
319 Western Reserve University and University Hospitals Cleveland Medical Center. Only de-
320 identified human specimens were collected and used for this work.

321

322 **Cell cultures and 3-D organotypic cultures**

323 The J1.1 cell line was obtained from the NIH AIDS Reagent Program. C22G cells were obtained
324 from Dr. Karn (Case Western Reserve University). Jurkat cells were purchased from American
325 Type Culture Collection (TIB-152, ATCC, Manassas, VA). These cells were maintained in
326 RPMI1640 medium (HyClone Lab., Inc., Logan, UT) supplemented with 10% exosome-depleted
327 FBS, which was prepared by ultracentrifugation of FBS (ThermoFisher Scientific, Waltham,
328 MA) at $100,000 \times g$ for 16 h at 4 °C [26], followed by collecting supernatants without disturbing
329 the pellet. Primary human oral epithelial cells (HOECs) were isolated from healthy patients who
330 underwent third-molar extraction at School of Dental Medicine as previously described [60].
331 HOECs and immortalized OKF6/TERT2 human oral keratinocytes were maintained as
332 previously described [31,61]. EpiOral™ oral mucosal tissues were purchased from MatTek Co.
333 (Ashland, MA), which consist of normal human oral keratinocytes that are differentiated into
334 tissues with a non-cornified, buccal phenotype. The 3-D organotypic cultures were constructed
335 following previously published protocols by Dongari-Bagtzoglou and Kashleva [35]. Briefly,
336 collagen gel cushion was prepared on ice from rat-tail type I collagen (Cat# Corning 354249,
337 Thermo-Fisher) supplemented with 10% FBS in DMEM and antibiotics. Fibroblast gel layer was
338 prepared by mixing 1 ml of NIH3T3 cells with the collagen gel as mentioned above. Culture
339 inserts containing gel cushion and fibroblast gel layer were cultured for 4 day, followed by
340 addition of OKF6/TERT6 cells to the center of the insert and cultured for 3 days. These inserts
341 were then lifted and cultured in airlifting medium for 14 days with change of the medium every
342 other day.

343

344 **Preparation of KSHV virions and EVs**

345 EVs were prepared from cell supernatants by differential ultracentrifugation with filtration steps
346 [26]. Briefly, cell culture media were centrifuged at $400 \times g$ for 5 min to remove cells, followed

347 by centrifugation at $11,000 \times g$ for 10 min to remove any possible apoptotic bodies and large cell
348 debris. EVs were precipitated at $100,000 \times g$ for 90 min at 4°C (50.2Ti rotor, Beckman Coulter,
349 Brea, CA) and suspended in PBS. Isolated EVs were quantified using the acetylcholinesterase
350 (AChE) assay system [26] (System Biosci. Inc/SBI, Palo Alto, CA) and maintained at -80°C in
351 DMEM for later use. To purify EVs from saliva, 2 ml of saliva was centrifuged at $400 \times g$ for 15
352 min to remove cell contaminants. After centrifugation at $11,000 \times g$ for 10 min, saliva EVs were
353 pelleted by ultracentrifugation at $100,000 \times g$ for 90 min at 4°C (Optima™ Max-XP, Beckman
354 Coulter). The EVs were washed in 2 ml PBS and pelleted again at $100,000 \times g$ for 90 min and
355 suspended in PBS. Saliva EVs were quantified using BCA assays to measure total EV proteins
356 following the manufacture's protocol (SBI).

357

358 **Flow cytometry analysis**

359 OKF6/TERT or HOECs were washed 3 times with PBS, then suspended in $100 \mu\text{l}$ of PBS. Flow
360 cytometric analysis was performed by Green Fluorescent Protein (GFP) on FACSaria Flow
361 Cytometer (BD Biosciences). FACS data was analyzed with FlowJo software (TreeStar Inc.).

362

363 **RT-PCR and immunoblot**

364 Total RNA was isolated and purified using High Pure RNA Isolation Kit (Roche) according to
365 the manufacturer's instructions. Extracted RNA was reverse-transcribed to cDNA (High-
366 Capacity cDNA Reverse Transcription, Applied Biosystems). Regular PCR analysis was
367 performed using Q5 Hot Start High-Fidelity 2x Master Mix (New England Biolabs) and detected
368 by the T100™ Thermal Cycler (Bio-Rad). Sequences of primers are listed in *SI Appendix* table
369 S1. For immunoblotting, total EV proteins were purified using the Total Exosome RNA &
370 Protein Isolation Kit (ThermoFisher) following the manufacturer's instructions. To prepare total
371 cellular proteins, cells were washed with PBS and then cellular lysates were obtained by adding
372 $300 \mu\text{l}$ of RIPA Lysis and Extraction Buffer (ThermoFisher). Protein lysates were separated by
373 SDS-PAGE and then transferred onto polyvinylidene fluoride membranes (PVDF, Merck

374 Millipore) for immunoblot analysis. Antibodies used in immunoblotting are listed in S4 Table.
375 Protein detection was performed by chemiluminescence using an ECL kit (ThermoFisher) with
376 the ChemiDoc XRS+ Imaging System (Bio-Rad).

377

378 **Immunofluorescence microscopy**

379 Immunofluorescence microscopy of 3-D cultures were performed as previously described [62]
380 with minor modifications. Briefly, each section (5 μm) was de-paraffinized 3 times in Clear-
381 Rite™ 3 and hydrated with 100% Alcohol followed by 95% Alcohol. Samples were blocked
382 with 10% donkey serum at room temperature for 1 hr. Each section was incubated with the
383 primary antibody at 4°C overnight. After washing in PBS, sections were stained with the
384 appropriate AlexaFluor-conjugated secondary antibody to the species of the primary antibody.
385 Sections were then mounted with the VECTASHIELD Fluorescent Mounting Media (Vector Lab
386 Inc., Burlingame, CA) containing DAPI to visualize nuclei. Immunofluorescent images were
387 generated using AMG EVOS FL digital inverted fluorescence microscope (AMG, Mill Creek,
388 WA). Confocal images were acquired with a Leica TCS SP8 system (Leica Microsystems) using
389 a 63 \times /1.4 objective at a pixel size of 90 nm. Channels were acquired sequentially by line. For
390 immunocytochemistry, cells on 8 well culture slide were fixed with 100% methanol at -20°C for
391 20 minutes followed by permeabilization with 0.3% Triton X-100 in PBS. Cells were then
392 stained with the primary antibody followed by incubation with appropriate secondary antibodies.
393 Fluorescent images were taken as described above. Antibodies for immunofluorescence
394 microscopy are listed in S5 Table.

395

396 **Statistics**

397 Results of treatments were compared with those of respective controls. Data are represented as
398 mean \pm S.D. Flow cytometry data were subjected to one-way ANOVA when sample sizes were
399 $n \leq 3$. Statistical significance was considered at $p < 0.05$. For data with $n \leq 5$, F-test was applied.
400 Data analyses were performed and graphs were generated using Prism (GraphPad Software, La
401 Jolla, CA) and Excel 2013 (Microsoft).

402

403 **Acknowledgments**

404 We thank the Light Microscopy Image Core at Case Western Reserve University School
405 of Medicine, supported by the NIH Office of Research Infrastructure Program Grant (S10-
406 OD024996), and the Cytometry & Imaging Microscope Shared Resources at the Case
407 Comprehensive Cancer Center, supported in part by the NIH/National Cancer Institute (NCI)
408 grant (P30CA043703), for technical assists. The following reagents were obtained through the
409 National Institute of Health (NIH) AIDS Reagent Program, Division of AIDS, National Institute
410 of Allergy and Infectious Diseases (NIAID), NIH: HIV-1 LAV infected Jurkat E6 cells (J1.1)
411 from Dr. Thomas Folks.

412

413 **References**

414

- 415 1. Chang Y, Cesarman E, Pessin MS, Lee F, Culpepper J, et al. (1994) Identification of
416 herpesvirus-like DNA sequences in AIDS-associated Kaposi's sarcoma. *Science* 266:
417 1865-1869.
- 418 2. Yarchoan R, Uldrick TS (2018) HIV-Associated Cancers and Related Diseases. *N Engl J Med*
419 378: 1029-1041.
- 420 3. Cannon MJ, Pellett PE (2002) Relationship between Kaposi sarcoma-associated herpesvirus
421 and HIV. *JAMA* 287: 1526; author reply 1527-1528.

- 422 4. Minhas V, Wood C (2014) Epidemiology and transmission of Kaposi's sarcoma-associated
423 herpesvirus. *Viruses* 6: 4178-4194.
- 424 5. Pauk J, Huang ML, Brodie SJ, Wald A, Koelle DM, et al. (2000) Mucosal shedding of human
425 herpesvirus 8 in men. *N Engl J Med* 343: 1369-1377.
- 426 6. Webster-Cyriaque J, Duus K, Cooper C, Duncan M (2006) Oral EBV and KSHV infection in
427 HIV. *Adv Dent Res* 19: 91-95.
- 428 7. Vannata B, Zucca E (2014) Hepatitis C virus-associated B-cell non-Hodgkin lymphomas.
429 *Hematology Am Soc Hematol Educ Program* 2014: 590-598.
- 430 8. Bender Ignacio RA, Goldman JD, Magaret AS, Selke S, Huang ML, et al. (2016) Patterns of
431 human herpesvirus-8 oral shedding among diverse cohorts of human herpesvirus-8
432 seropositive persons. *Infect Agent Cancer* 11: 7.
- 433 9. Dittmer DP, Tamburro K, Chen H, Lee A, Sanders MK, et al. (2017) Oral shedding of
434 herpesviruses in HIV-infected patients with varying degrees of immune status. *AIDS* 31:
435 2077-2084.
- 436 10. Facciola A, Venanzi Rullo E, Ceccarelli M, D'Aleo F, Di Rosa M, et al. (2017) Kaposi's
437 sarcoma in HIV-infected patients in the era of new antiretrovirals. *Eur Rev Med*
438 *Pharmacol Sci* 21: 5868-5869.
- 439 11. Hesamizadeh K, Keyvani H, Bokharaei-Salim F, Monavari SH, Esghaei M, et al. (2016)
440 Molecular Epidemiology of Kaposi's Sarcoma-Associated Herpes Virus, and Risk
441 Factors in HIV-infected Patients in Tehran, 2014. *Iran Red Crescent Med J* 18: e32603.
- 442 12. Labo N, Miley W, Benson CA, Campbell TB, Whitby D (2015) Epidemiology of Kaposi's
443 sarcoma-associated herpesvirus in HIV-1-infected US persons in the era of combination
444 antiretroviral therapy. *AIDS* 29: 1217-1225.
- 445 13. Colombo M, Raposo G, Thery C (2014) Biogenesis, secretion, and intercellular interactions
446 of exosomes and other extracellular vesicles. *Annu Rev Cell Dev Biol* 30: 255-289.
- 447 14. Kulkarni R, Prasad A (2017) Exosomes Derived from HIV-1 Infected DCs Mediate Viral
448 trans-Infection via Fibronectin and Galectin-3. *Sci Rep* 7: 14787.
- 449 15. Madison MN, Okeoma CM (2015) Exosomes: Implications in HIV-1 Pathogenesis. *Viruses*
450 7: 4093-4118.
- 451 16. Palanisamy V, Sharma S, Deshpande A, Zhou H, Gimzewski J, et al. (2010) Nanostructural
452 and transcriptomic analyses of human saliva derived exosomes. *PLoS One* 5: e8577.

- 453 17. Harding C, Heuser J, Stahl P (1983) Receptor-mediated endocytosis of transferrin and
454 recycling of the transferrin receptor in rat reticulocytes. *J Cell Biol* 97: 329-339.
- 455 18. Harding CV, Heuser JE, Stahl PD (2013) Exosomes: looking back three decades and into the
456 future. *J Cell Biol* 200: 367-371.
- 457 19. Edgar JR (2016) Q&A: What are exosomes, exactly? *BMC Biol* 14: 46.
- 458 20. Tkach M, Thery C (2016) Communication by Extracellular Vesicles: Where We Are and
459 Where We Need to Go. *Cell* 164: 1226-1232.
- 460 21. Al-Nedawi K, Meehan B, Micallef J, Lhotak V, May L, et al. (2008) Intercellular transfer of
461 the oncogenic receptor EGFRvIII by microvesicles derived from tumour cells. *Nat Cell*
462 *Biol* 10: 619-624.
- 463 22. Yanez-Mo M, Siljander PR, Andreu Z, Zavec AB, Borrás FE, et al. (2015) Biological
464 properties of extracellular vesicles and their physiological functions. *J Extracell Vesicles*
465 4: 27066.
- 466 23. Kowal J, Arras G, Colombo M, Jouve M, Morath JP, et al. (2016) Proteomic comparison
467 defines novel markers to characterize heterogeneous populations of extracellular vesicle
468 subtypes. *Proc Natl Acad Sci U S A* 113: E968-977.
- 469 24. Narayanan A, Iordanskiy S, Das R, Van Duyne R, Santos S, et al. (2013) Exosomes derived
470 from HIV-1-infected cells contain trans-activation response element RNA. *J Biol Chem*
471 288: 20014-20033.
- 472 25. Berkhout B, Silverman RH, Jeang KT (1989) Tat trans-activates the human
473 immunodeficiency virus through a nascent RNA target. *Cell* 59: 273-282.
- 474 26. Chen L, Feng Z, Yue H, Bazdar D, Mbonye U, et al. (2018) Exosomes derived from HIV-1-
475 infected cells promote growth and progression of cancer via HIV TAR RNA. *Nat*
476 *Commun* 9: 4585.
- 477 27. Sampey GC, Saifuddin M, Schwab A, Barclay R, Punya S, et al. (2016) Exosomes from
478 HIV-1-infected Cells Stimulate Production of Pro-inflammatory Cytokines through
479 Trans-activating Response (TAR) RNA. *J Biol Chem* 291: 1251-1266.
- 480 28. Naslund TI, Paquin-Proulx D, Paredes PT, Vallhov H, Sandberg JK, et al. (2014) Exosomes
481 from breast milk inhibit HIV-1 infection of dendritic cells and subsequent viral transfer to
482 CD4+ T cells. *AIDS* 28: 171-180.

- 483 29. Madison MN, Roller RJ, Okeoma CM (2014) Human semen contains exosomes with potent
484 anti-HIV-1 activity. *Retrovirology* 11: 102.
- 485 30. Brulois KF, Chang H, Lee AS, Ensser A, Wong LY, et al. (2012) Construction and
486 manipulation of a new Kaposi's sarcoma-associated herpesvirus bacterial artificial
487 chromosome clone. *J Virol* 86: 9708-9720.
- 488 31. Dickson MA, Hahn WC, Ino Y, Ronfard V, Wu JY, et al. (2000) Human keratinocytes that
489 express hTERT and also bypass a p16(INK4a)-enforced mechanism that limits life span
490 become immortal yet retain normal growth and differentiation characteristics. *Mol Cell*
491 *Biol* 20: 1436-1447.
- 492 32. Perez VL, Rowe T, Justement JS, Butera ST, June CH, et al. (1991) An HIV-1-infected T
493 cell clone defective in IL-2 production and Ca²⁺ mobilization after CD3 stimulation. *J*
494 *Immunol* 147: 3145-3148.
- 495 33. Miller CS, Berger JR, Mootoor Y, Avdiushko SA, Zhu H, et al. (2006) High prevalence of
496 multiple human herpesviruses in saliva from human immunodeficiency virus-infected
497 persons in the era of highly active antiretroviral therapy. *J Clin Microbiol* 44: 2409-2415.
- 498 34. They C, Witwer KW, Aikawa E, Alcaraz MJ, Anderson JD, et al. (2018) Minimal
499 information for studies of extracellular vesicles 2018 (MISEV2018): a position statement
500 of the International Society for Extracellular Vesicles and update of the MISEV2014
501 guidelines. *J Extracell Vesicles* 7: 1535750.
- 502 35. Dongari-Bagtzoglou A, Kashleva H (2006) Development of a highly reproducible three-
503 dimensional organotypic model of the oral mucosa. *Nat Protoc* 1: 2012-2018.
- 504 36. Das SR, Jameel S (2005) Biology of the HIV Nef protein. *Indian J Med Res* 121: 315-332.
- 505 37. Rice AP (2017) The HIV-1 Tat Protein: Mechanism of Action and Target for HIV-1 Cure
506 Strategies. *Curr Pharm Des* 23: 4098-4102.
- 507 38. Pearson R, Kim YK, Hokello J, Lassen K, Friedman J, et al. (2008) Epigenetic silencing of
508 human immunodeficiency virus (HIV) transcription by formation of restrictive chromatin
509 structures at the viral long terminal repeat drives the progressive entry of HIV into
510 latency. *J Virol* 82: 12291-12303.
- 511 39. Kulinski T, Olejniczak M, Huthoff H, Bielecki L, Pachulska-Wieczorek K, et al. (2003) The
512 apical loop of the HIV-1 TAR RNA hairpin is stabilized by a cross-loop base pair. *J Biol*
513 *Chem* 278: 38892-38901.

- 514 40. Duconge F, Toulme JJ (1999) In vitro selection identifies key determinants for loop-loop
515 interactions: RNA aptamers selective for the TAR RNA element of HIV-1. *RNA* 5: 1605-
516 1614.
- 517 41. Choi BH, Choi JS, Rhie DJ, Yoon SH, Min DS, et al. (2002) Direct inhibition of the cloned
518 Kv1.5 channel by AG-1478, a tyrosine kinase inhibitor. *Am J Physiol Cell Physiol* 282:
519 C1461-1468.
- 520 42. Hwang S, Gwack Y, Byun H, Lim C, Choe J (2001) The Kaposi's sarcoma-associated
521 herpesvirus K8 protein interacts with CREB-binding protein (CBP) and represses CBP-
522 mediated transcription. *J Virol* 75: 9509-9516.
- 523 43. Liu D, Wang Y, Yuan Y (2018) Kaposi's Sarcoma-Associated Herpesvirus K8 Is an RNA
524 Binding Protein That Regulates Viral DNA Replication in Coordination with a
525 Noncoding RNA. *J Virol* 92.
- 526 44. Citri A, Yarden Y (2006) EGF-ERBB signalling: towards the systems level. *Nat Rev Mol*
527 *Cell Biol* 7: 505-516.
- 528 45. Lemmon MA, Schlessinger J, Ferguson KM (2014) The EGFR family: not so prototypical
529 receptor tyrosine kinases. *Cold Spring Harb Perspect Biol* 6: a020768.
- 530 46. Arvelo F, Sojo F, Cotte C (2016) Tumour progression and metastasis. *Ecancermedicallscience*
531 10: 617.
- 532 47. Angeletti PC, Zhang L, Wood C (2008) The viral etiology of AIDS-associated malignancies.
533 *Adv Pharmacol* 56: 509-557.
- 534 48. Grulich AE, van Leeuwen MT, Falster MO, Vajdic CM (2007) Incidence of cancers in
535 people with HIV/AIDS compared with immunosuppressed transplant recipients: a meta-
536 analysis. *Lancet* 370: 59-67.
- 537 49. Hernandez-Ramirez RU, Shiels MS, Dubrow R, Engels EA (2017) Cancer risk in HIV-
538 infected people in the USA from 1996 to 2012: a population-based, registry-linkage study.
539 *Lancet HIV* 4: e495-e504.
- 540 50. Duus KM, Lentchitsky V, Wagenaar T, Grose C, Webster-Cyriaque J (2004) Wild-type
541 Kaposi's sarcoma-associated herpesvirus isolated from the oropharynx of immune-
542 competent individuals has tropism for cultured oral epithelial cells. *J Virol* 78: 4074-4084.

- 543 51. Morris TL, Arnold RR, Webster-Cyriaque J (2007) Signaling cascades triggered by bacterial
544 metabolic end products during reactivation of Kaposi's sarcoma-associated herpesvirus. *J*
545 *Virol* 81: 6032-6042.
- 546 52. Yu X, Shahir AM, Sha J, Feng Z, Eapen B, et al. (2014) Short-chain fatty acids from
547 periodontal pathogens suppress histone deacetylases, EZH2, and SUV39H1 to promote
548 Kaposi's sarcoma-associated herpesvirus replication. *J Virol* 88: 4466-4479.
- 549 53. Kolb G, Reigadas S, Castanotto D, Faure A, Ventura M, et al. (2006) Endogenous expression
550 of an anti-TAR aptamer reduces HIV-1 replication. *RNA Biol* 3: 150-156.
- 551 54. Upert G, Di Giorgio A, Upadhyay A, Manvar D, Pandey N, et al. (2012) Inhibition of HIV
552 Replication by Cyclic and Hairpin PNAs Targeting the HIV-1 TAR RNA Loop. *J*
553 *Nucleic Acids* 2012: 591025.
- 554 55. Koumanov F, Holman GD (2007) Thrifty Tbc1d1 and Tbc1d4 proteins link signalling and
555 membrane trafficking pathways. *Biochem J* 403: e9-11.
- 556 56. Saraya R, Veenhuis M, van der Klei IJ (2010) Peroxisomes as dynamic organelles:
557 peroxisome abundance in yeast. *FEBS J* 277: 3279-3288.
- 558 57. Davis CD, Johnson WT (2002) Dietary copper affects azoxymethane-induced intestinal
559 tumor formation and protein kinase C isozyme protein and mRNA expression in colon of
560 rats. *J Nutr* 132: 1018-1025.
- 561 58. Ye F, Karn J (2015) Bacterial Short Chain Fatty Acids Push All The Buttons Needed To
562 Reactivate Latent Viruses. *Stem Cell Epigenet* 2.
- 563 59. Sun R, Tan X, Wang X, Wang X, Yang L, et al. (2017) Epigenetic Landscape of Kaposi's
564 Sarcoma-Associated Herpesvirus Genome in Classic Kaposi's Sarcoma Tissues. *PLoS*
565 *Pathog* 13: e1006167.
- 566 60. Krisanaprakornkit S, Kimball JR, Weinberg A, Darveau RP, Bainbridge BW, et al. (2000)
567 Inducible expression of human beta-defensin 2 by *Fusobacterium nucleatum* in oral
568 epithelial cells: multiple signaling pathways and role of commensal bacteria in innate
569 immunity and the epithelial barrier. *Infect Immun* 68: 2907-2915.
- 570 61. Kawsar HI, Weinberg A, Hirsch SA, Venizelos A, Howell S, et al. (2009) Overexpression of
571 human beta-defensin-3 in oral dysplasia: potential role in macrophage trafficking. *Oral*
572 *Oncol* 45: 696-702.

573 62. Jin G, Kawsar HI, Hirsch SA, Zeng C, Jia X, et al. (2010) An antimicrobial peptide regulates
574 tumor-associated macrophage trafficking via the chemokine receptor CCR2, a model for
575 tumorigenesis. PLoS One 5: e10993.

576

577 **Supporting information**

578 **S1 Fig. Titration of KSHV infection in immortalized OKF6/TERT2 cells.** OKF6/TERT2
579 cells were grown in 6-well plates to 70-80% confluency and then were added with KSHV virions
580 at different dilutions. After 20 hr incubations, cells were washed with PBS and fixed in methanol
581 at 4 °C for 30 min. Immunofluorescence microscopy was performed using antibodies to KSHV
582 LANA and GFP. Red, LANA; green, GFP; blue, nuclei.

583

584 **S2 Fig. Fig. S2. Inhibition of KSHV infection enhanced by HIV+ EVs by cetuximab.**
585 OKF6/TERT2 cells were treated with EVs from Jurkat and HIV+ J1.1 T cells (4×10^9 EVs ml⁻¹),
586 or remained un-treated, in the presence or absence of cetuximab (20 µg ml⁻¹), followed by
587 addition of KSHV virions. Microphotographs of GFP+ cells were taken 20 hr after KSHV
588 infection.

589

590 **S3 Table. Total proteins from EV stocks prepared from various volumes of the saliva**

591 **S4 Table. Primers used in this report**

592 **S5 Table. Antibodies used in this report**

593

594

595

596

597

598

599

600 **Figures and figure legends**

601

602 **Fig 1. HIV+ EVs promote KSHV infection in oral epithelial cells.** (A) OKF6/TERT2 cells were treated
603 with EVs from J1.1 (HIV+) or Jurkat (HIV-) cells at 4×10^9 EVs ml⁻¹ [34], followed by KSHV infection
604 for 20 hr. Cells were fixed for immunofluorescent staining using antibodies to LANA and GFP. (B) Flow
605 cytometry of GFP+ cells after KSHV infection in the presence of EVs from J1.1 and Jurkat cells,
606 respectively. Ctrl, KSHV alone. Data represent one independent experiment ($n=4$) out of three repeats. * p
607 <0.05 , F -test. (C) Flow cytometry histogram of (B).

608

609 **Fig 2. HIV+ EVs from saliva of HIV-infected donors promote KSHV infection in oral epithelial**
610 **cells.** (A) Immunoblots of total proteins extracted from saliva EVs from healthy (N1 and N3) and HIV+
611 (P8 and P9) individuals. Molecular weight for each protein indicated. (B) RT-PCR on total RNA
612 extracted from saliva EVs of healthy and HIV+ donors. M, DNA size marker. (C) OKF6/TERT2 cells
613 were treated with HIV+ (P8 and P9) and HIV- (N1 and N3) saliva EVs (100 μ g ml⁻¹), respectively, and
614 then infected with KSHV for 20 hr. Infection was quantified by GFP flow cytometry. *, $p<0.05$. (D)
615 LANA (red) and GFP (green) expression in primary human oral epithelial cells (HOECs) upon KSHV
616 infection using immunofluorescent staining. nuclei, blue (DAPI); representative images shown. (E)
617 HOECs were treated with saliva EVs (100 μ g ml⁻¹) from healthy (N1 and N3) and HIV+ (P8 and P9)
618 donors, followed by KSHV infection. KSHV-infected GFP+ HOECs were quantified using flow
619 cytometry. Data represent mean \pm S.D. *, $p<0.05$. (F). HOECs were treated with saliva EVs (100 μ g ml⁻¹)
620 purified from healthy ($n=4$) and HIV-infected donors ($n=8$), followed by KSHV infection. KSHV-
621 infected GFP+ HOECs were determined by flow cytometry. * $p <0.03$, one-way ANOVA. (G) Mean
622 fluorescence intensity plot of (F). * $p <0.04$, one-way ANOVA.

623

624 **Fig 3. KSHV infection is increased by HIV+ EVs in 3-D cultural models of oral epithelial**
625 **cells.** (A) Haemotoxylin and eosin (H&E) staining of the organotypic culture of OKF6/TERT2
626 cells (upper panel) and the oral buccal mucosal tissue consisting of primary human oral epithelial
627 cells (MetTak Inc.). Representative images shown. (B) HIV+ J1.1 T-cell EVs promote KSHV
628 infectivity in a 3-D organotypic culture model constructed using OKF6/TERT cells. GFP+ cells
629 represent KSHV-infected cells. Representative images shown. (C) The 3-D cultured oral buccal
630 mucosal tissues were treated with EVs from HIV-infected J1.1 and control Jurkat T cells,
631 respectively, followed by KSHV infection. Tissue sections were stained with antibodies to
632 LANA and GFP. Red, LANA; green, GFP; blue, nuclei. Arrows, GFP; arrowheads, LANA.
633 Representative images shown. (D) Quantification of LANA+ cells vs. total cells of (C). Data
634 represented mean \pm S.D.

635
636 **Fig 4. KSHV infection is enhanced by the HIV TAR RNA.** (A) Immunoblots of HIV Tat and
637 Nef proteins on total proteins extracted from EVs isolated from cultural supernatants of Jurkat,
638 J1.1 and C22G cells. Total cell lysates of J1.1 cells (J1.1 Cells) were used as control. (B)
639 Infection of KSHV in OKF6/TERT cells in the presence of EVs from Jurkat, C22G and J1.1 T
640 cells. GFP+ KSHV-infected cells were determined by flow cytometry. $n=3$; *, $p<0.05$; F -test. (C)
641 OKF6/TERT2 cells were transfected with synthetic HIV TAR RNA (TAR), the mutant TAR
642 RNA (mutTAR), TAR RNA together with the R06 aptamer (TAR+R06) or the scrambled
643 aptamer (TAR+Scrb), followed by KSHV infection for 20 hr. KSHV transfection was
644 determined by GFP flow cytometry. Data represent one independent experiment ($n=4$) out of
645 three repeats. * $p < 0.01$, ** $p < 0.02$, F -test.

646

647 **Fig 5. Increased KSHV infection by HIV+ EVs is EGFR dependent.** (A) KSHV infected in
648 OKF6/TERT2 cells in the presence of EVs from Jurkat or J1.1 cells (4×10^9 EVs ml⁻¹) with or
649 without cetuximab treatment (20 μ g ml⁻¹). Data (mean \pm S.D.) represent one independent
650 experiment ($n=3$) out of three repeats. * $p < 0.02$, F -test. (B) OKF6/TERT2 cells were pre-treated
651 with J1.1 and Jurkat EVs (4×10^9 ml⁻¹), respectively, in the presence or absence of cetuximab (Cet)
652 or AG1478 (2 μ m) for 30 min, followed by KSHV infection for 20 hr. Total protein lysates of
653 cells were used for immunoblotting on viral LANA and K8 proteins. (C) Flow cytometry of
654 GFP+ KSHV-infected OKF6/TERT2 cells treated with EVs from Jurkat and J1.1 cells treated
655 with or without cetuximab (20 μ g/ml). $n=3$; *, $p < 0.05$; F -test. (D) Oral buccal mucosal tissues
656 were treated with J1.1 or Jurkat cell EVs (4×10^9 EVs ml⁻¹) with or without cetuximab (cet),
657 followed by KSHV infection. Arrowheads, LANA; green, GFP; blue, nuclei.

658

659 **Fig 6. HIV+ EVs activate p38 MAPK via EGFR in oral epithelial cells.** (A) OKF6/TERT2
660 cells were pre-treated with cetuximab (Cet, 20 μ g ml⁻¹) or AG1478 (2 μ m) for 30 min, followed
661 by treatment with J1.1 and Jurkat EVs (4×10^9 EVs ml⁻¹), respectively, for 10 min. Total protein
662 lysates were used for immunoblotting. p-p38, phosphorylated p38; pY1173- and pY1068-EGFR,
663 phosphorylated EGFR at 1173 and 1069 tyrosine residues, respectively. EGF (10 ng ml⁻¹) was
664 used as positive control. (B) HOECs were treated with HIV+ J1.1 or control Jurkat EVs (4×10^9
665 ml⁻¹) for 10 min, followed by cellular lysis. Total cellular proteins were used for immunoblot.
666 EGF (10 ng ml⁻¹) treatment was used as a positive control.

bioRxiv preprint doi: <https://doi.org/10.1101/640532>; this version posted May 16, 2019. The copyright holder for this preprint (which was not certified by peer review) is the author/funder, who has granted bioRxiv a license to display the preprint in perpetuity. It is made available under aCC-BY 4.0 International license.

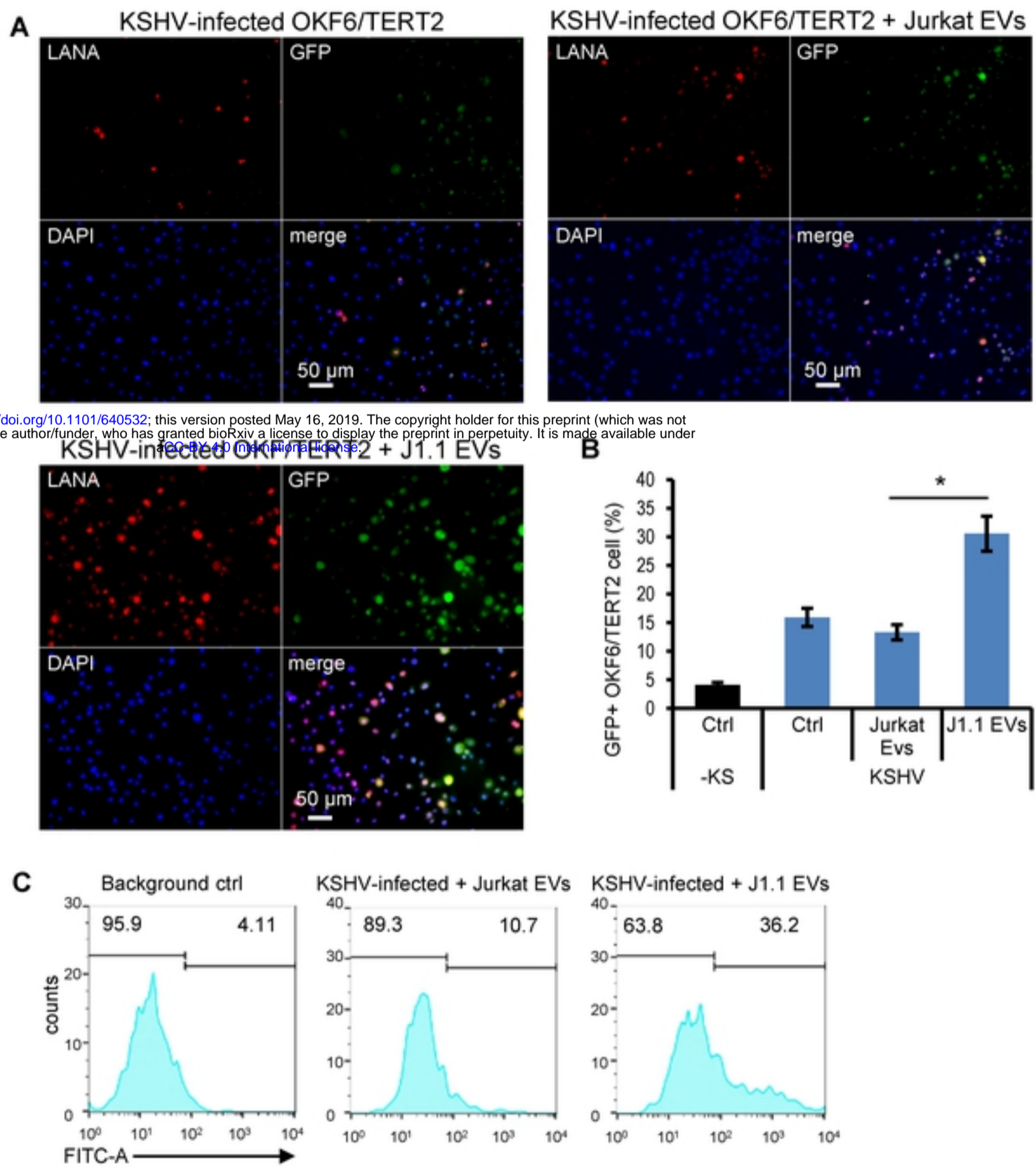


Fig1

bioRxiv preprint doi: <https://doi.org/10.1101/640532>; this version posted May 16, 2019. The copyright holder for this preprint (which was not certified by peer review) is the author/funder, who has granted bioRxiv a license to display the preprint in perpetuity. It is made available under aCC-BY 4.0 International license.

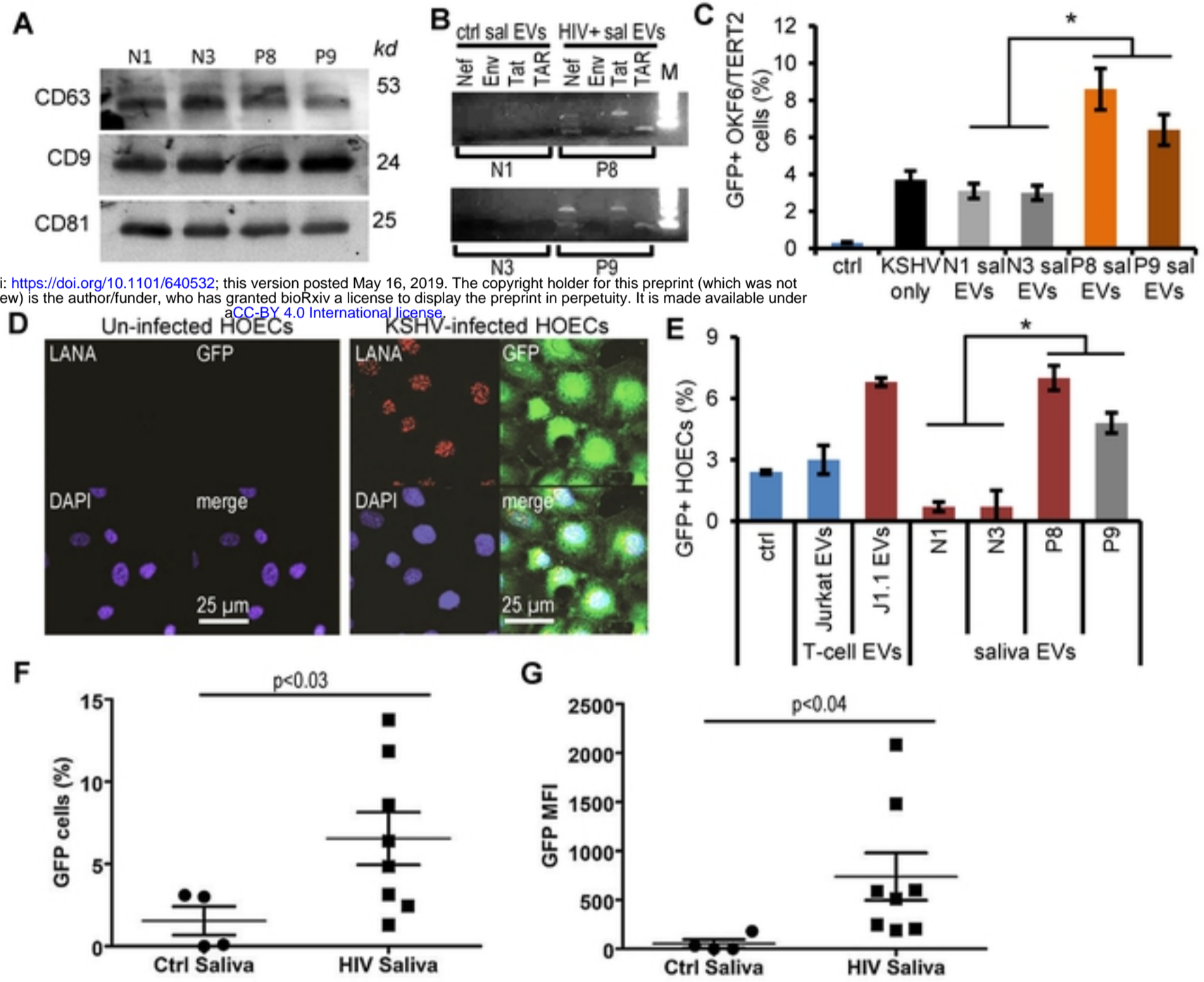
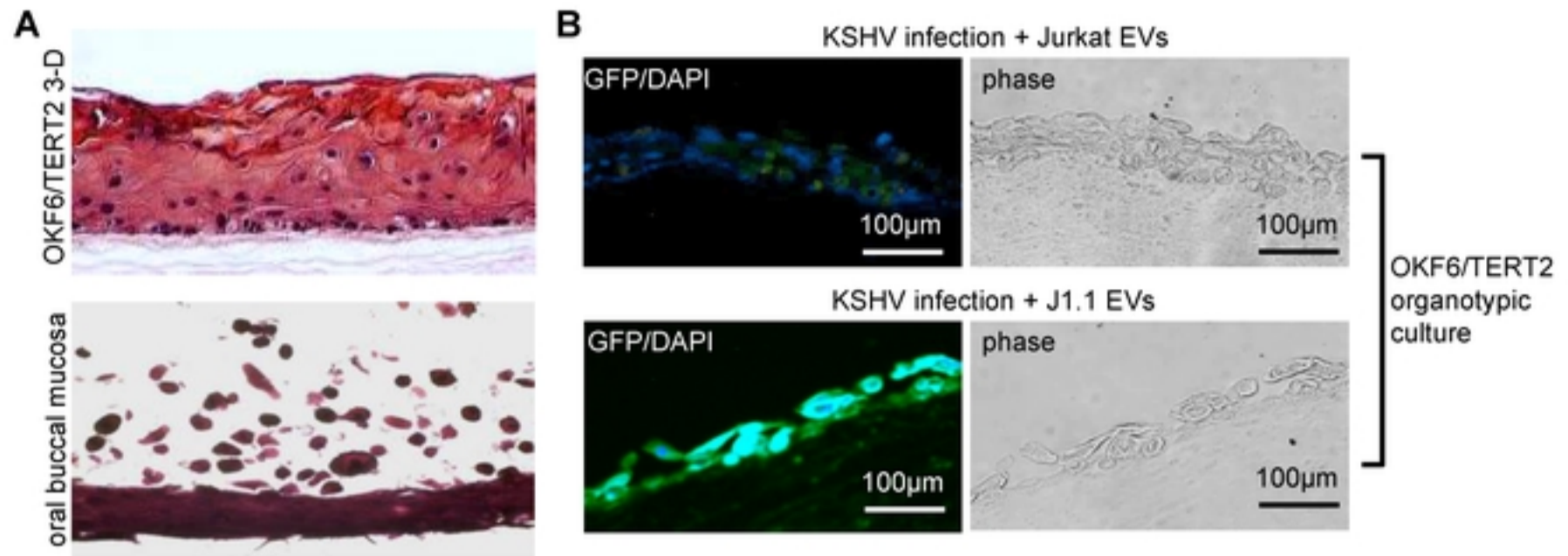
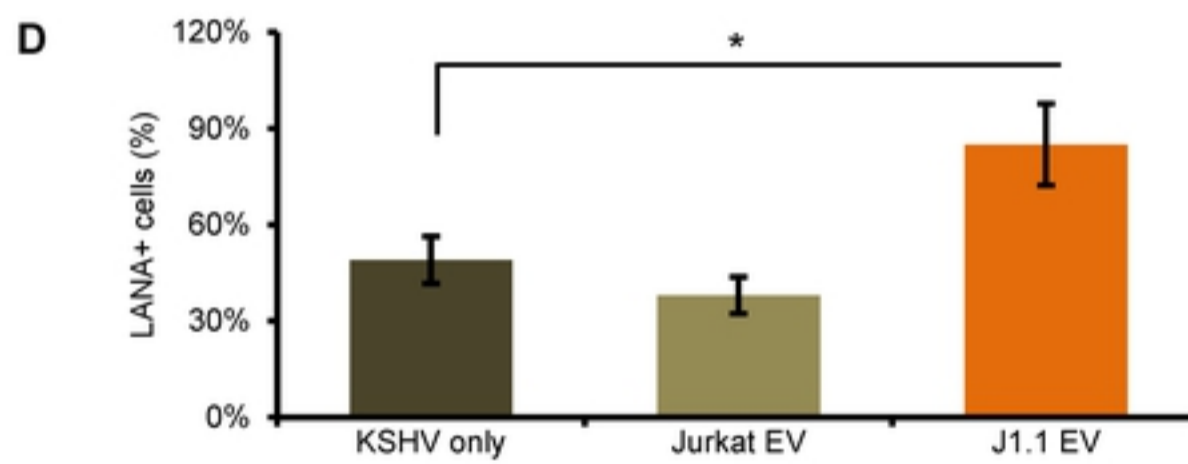
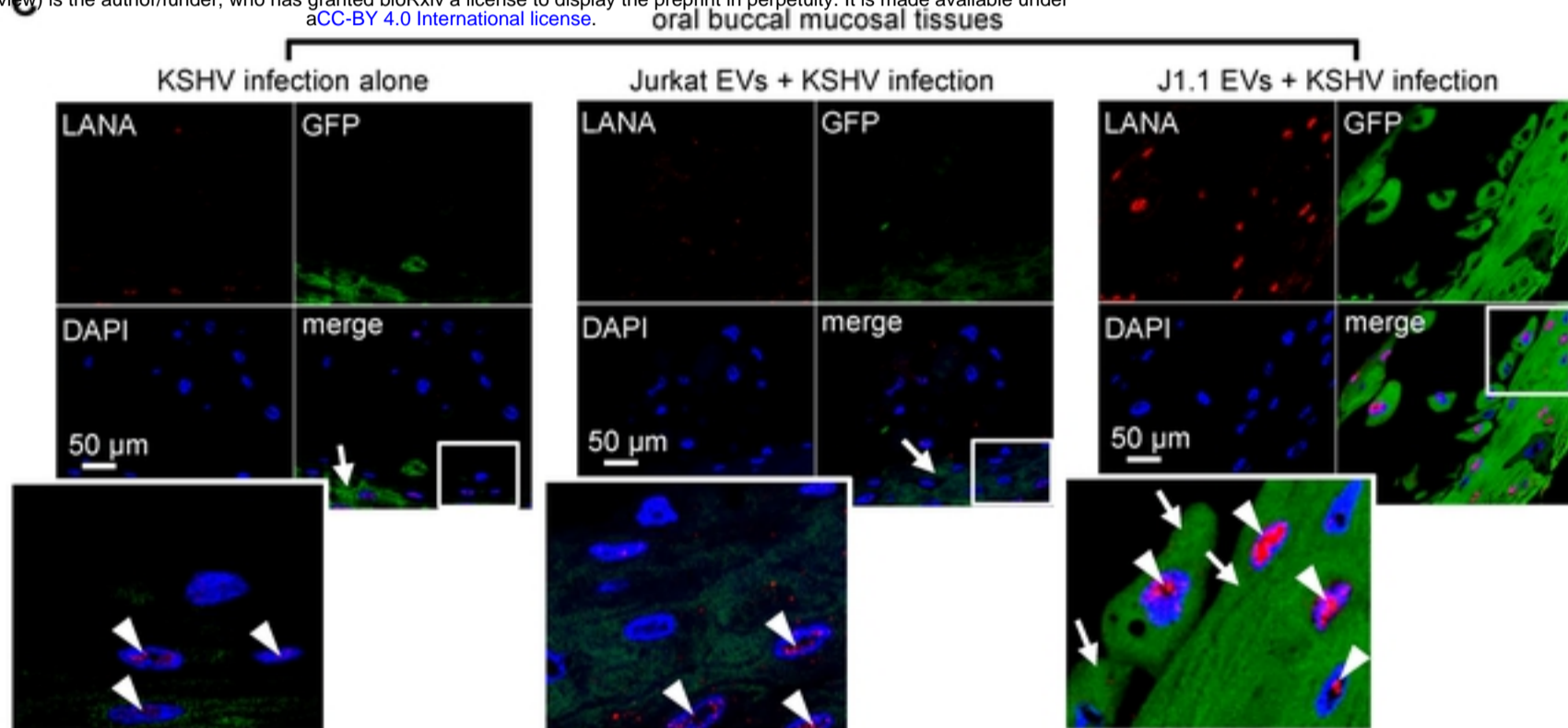


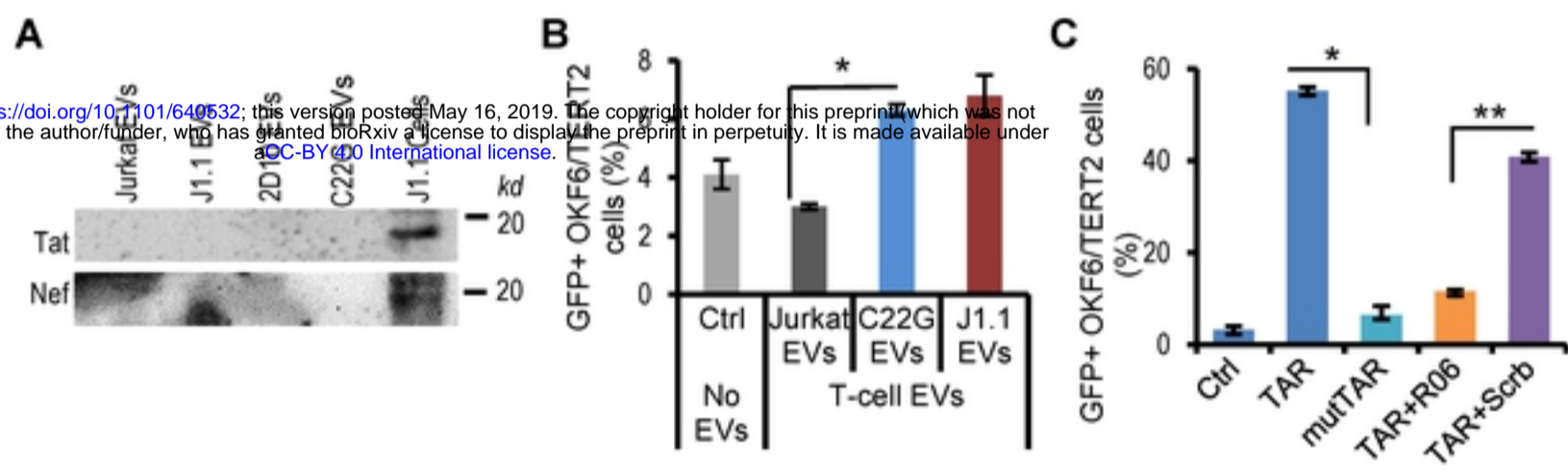
Fig2



bioRxiv preprint doi: <https://doi.org/10.1101/640532>; this version posted May 16, 2019. The copyright holder for this preprint (which was not certified by peer review) is the author/funder, who has granted bioRxiv a license to display the preprint in perpetuity. It is made available under aCC-BY 4.0 International license.



bioRxiv preprint doi: <https://doi.org/10.1101/640532>; this version posted May 16, 2019. The copyright holder for this preprint (which was not certified by peer review) is the author/funder, who has granted bioRxiv a license to display the preprint in perpetuity. It is made available under aCC-BY 4.0 International license.



bioRxiv preprint doi: <https://doi.org/10.1101/640532>; this version posted May 16, 2019. The copyright holder for this preprint (which was not certified by peer review) is the author/funder, who has granted bioRxiv a license to display the preprint in perpetuity. It is made available under aCC-BY 4.0 International license.

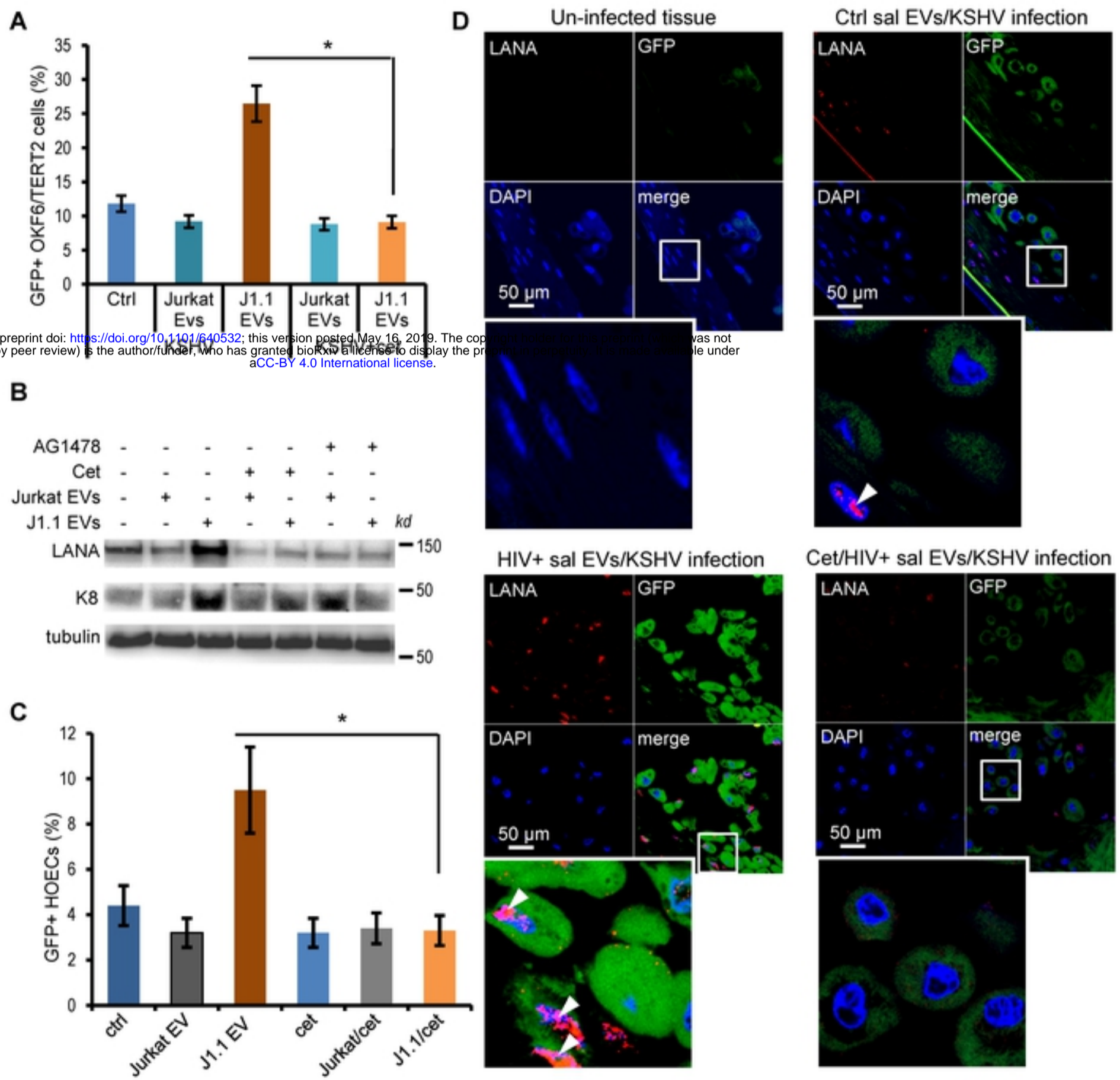


Fig5

bioRxiv preprint doi: <https://doi.org/10.1101/640532>; this version posted May 16, 2019. The copyright holder for this preprint (which was not certified by peer review) is the author/funder, who has granted bioRxiv a license to display the preprint in perpetuity. It is made available under aCC-BY 4.0 International license.

